Supporting Information

Bucket Effect on High-performance Li-O_2 Batteries Based on P-doped 3D NiO Microspheres with Conformal Growth of Discharge Products

Yuxin Long,[#a] Zidong Zhang,[#a] Lanling Zhao,[b] Qingxi Zeng,[c] Qiang Li,[c] Jun Wang,*[ac] Deyuan Li,[a] Qing Xia,[a] Yao Liu,*[a] Xue Han,[a] Zhaorui Zhou,[a] Yebing Li,[a] Yiming Zhang,[a] Shulei Chou*[d]

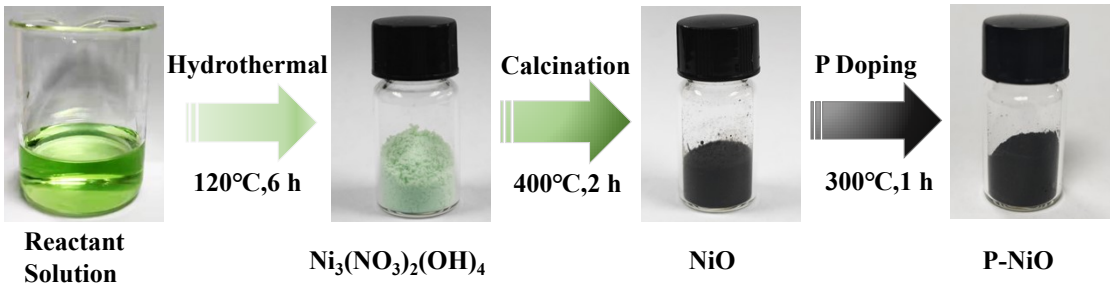

Fig. S1. Digital photo illustration of the synthesis path.

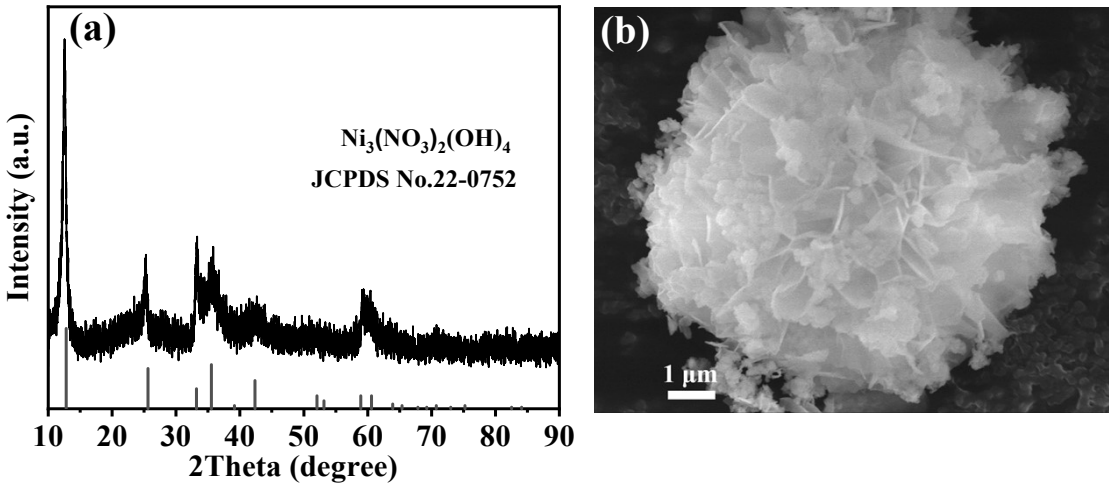

Fig. S2. (a) XRD pattern and (b) SEM image of NiO precursor.

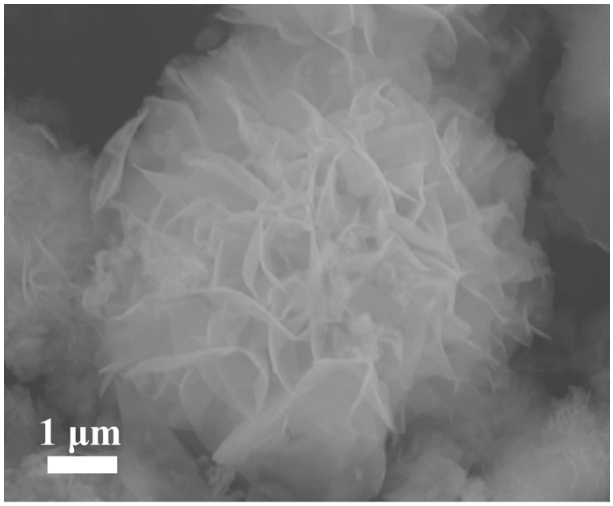

Fig. S3. SEM image of NiO.

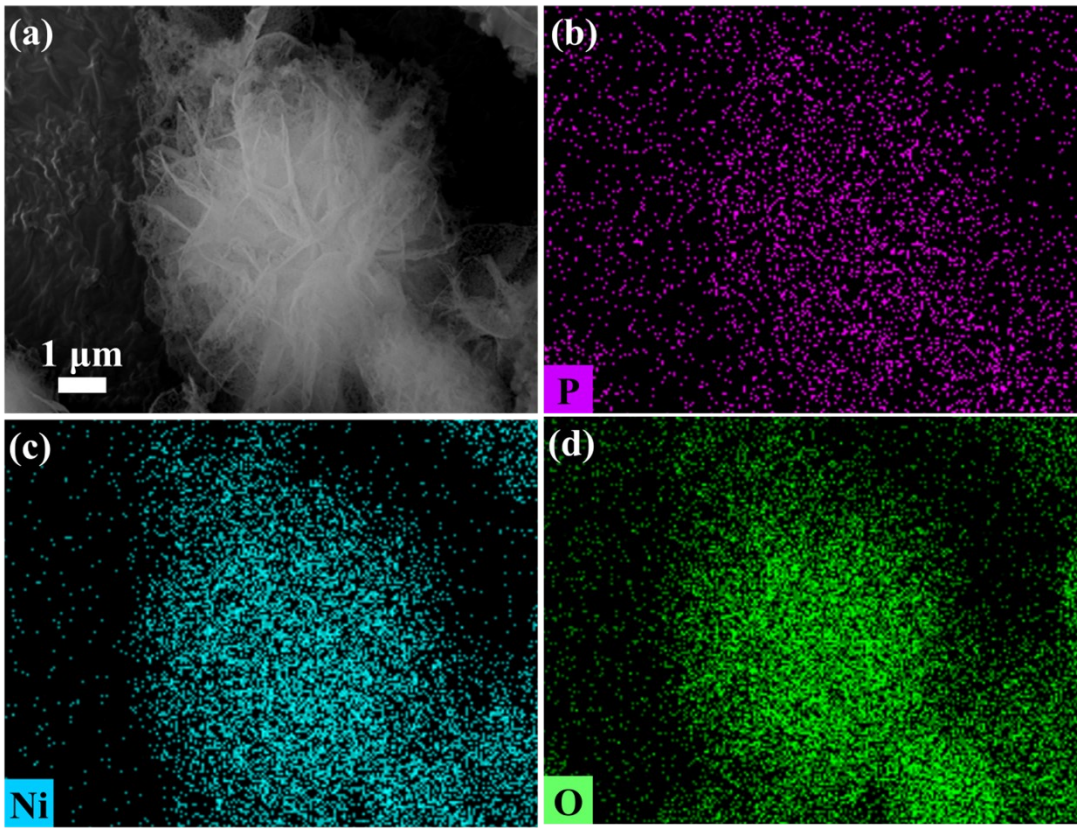

Fig. S4. SEM image with EDS patterns of 0.5P-NiO.

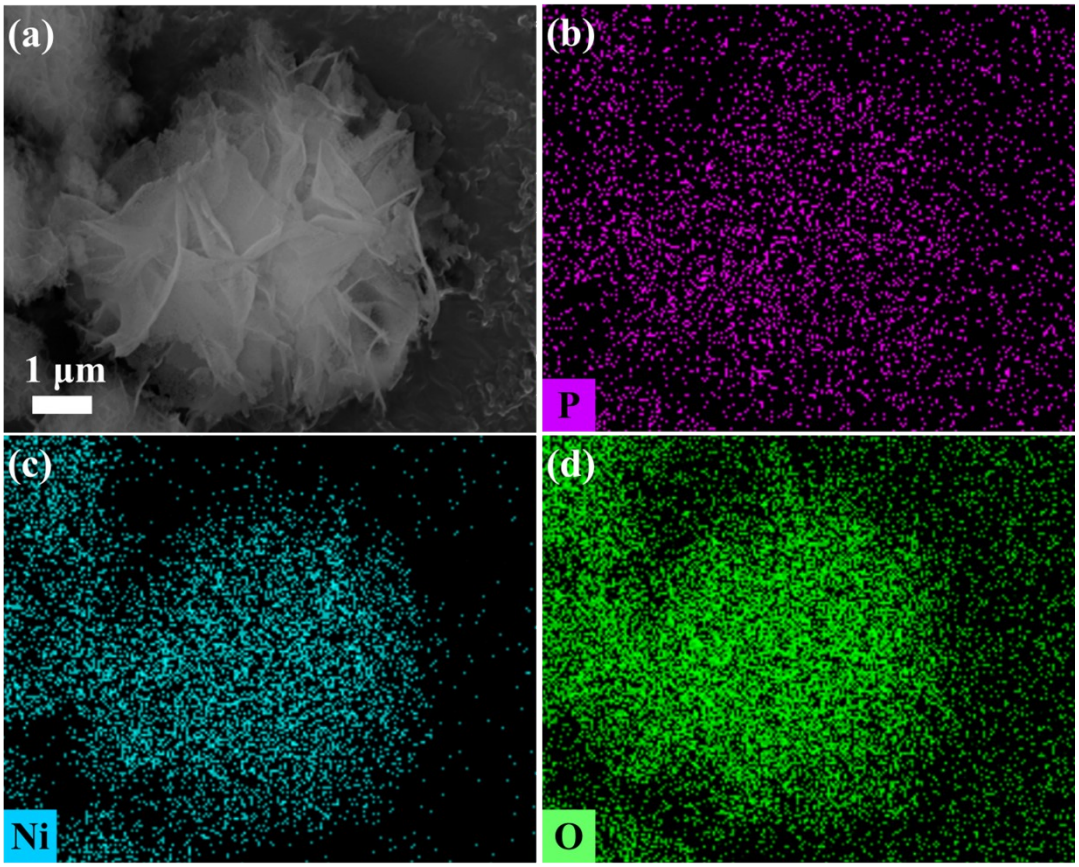

Fig. S5. SEM image with EDS patterns of 1P-NiO.

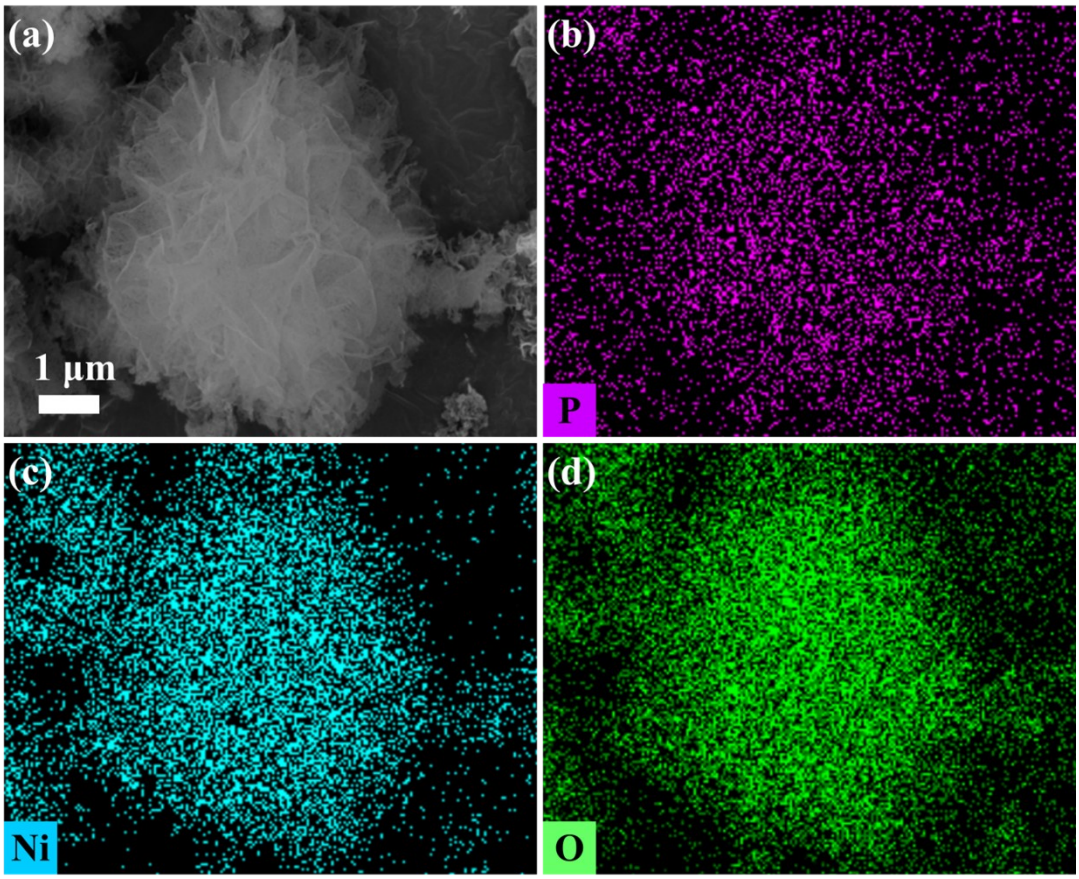

Fig. S6. SEM image with EDS patterns of 1.5P-NiO.

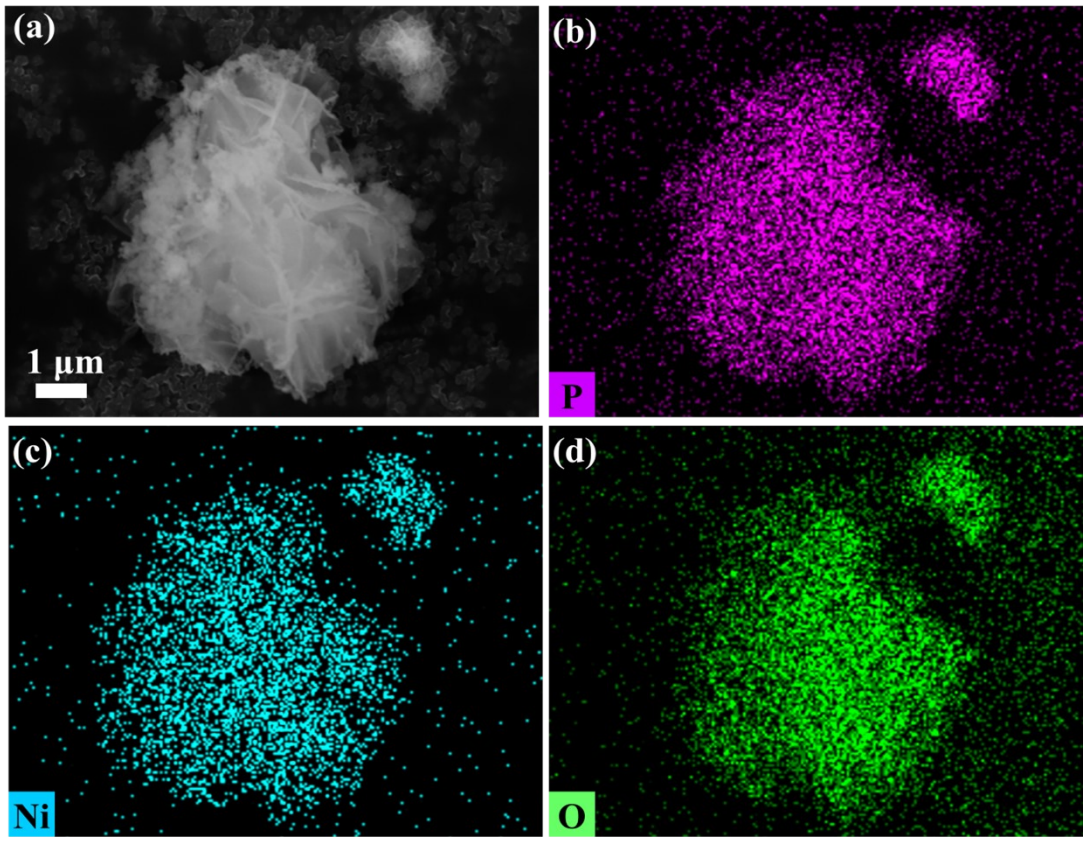

Fig. S7. SEM image with EDS patterns of 3P-NiO.

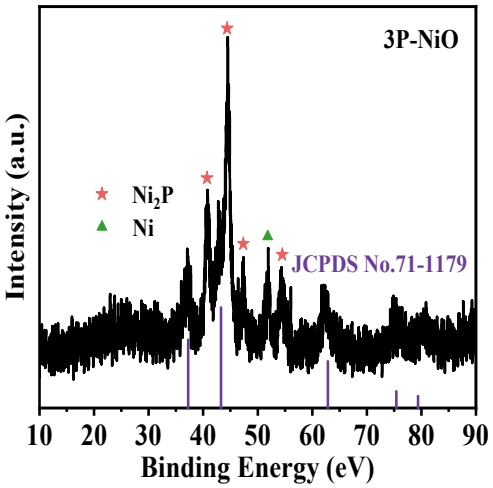

Fig. S8. XRD pattern of 3P-NiO.

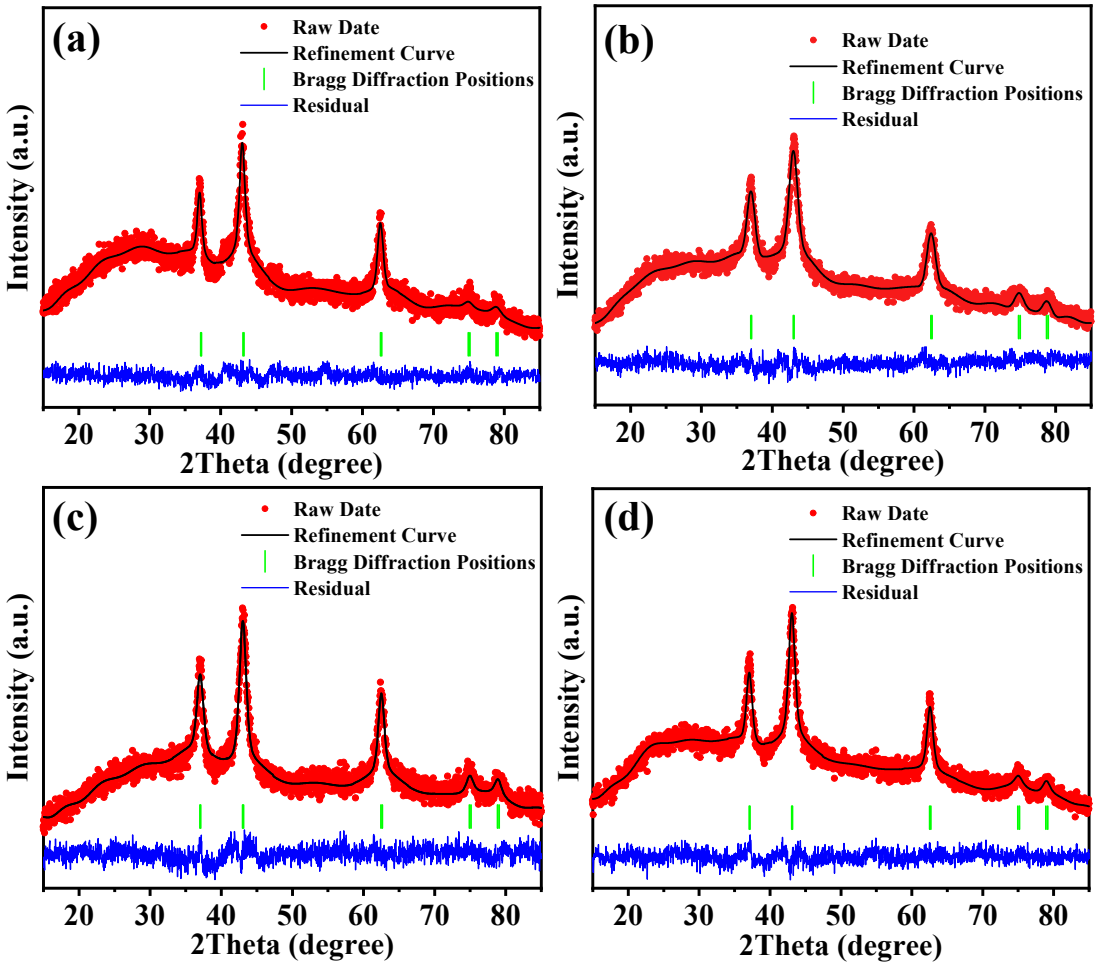

Fig. S9. Rietveld refined XRD patterns of (a) NiO, (b) 0.5P-NiO, (c)1P-NiO and (d)1.5P-NiO.

Table S1. Lattice parameters, cell volume, agreement factor, atomic coordinates, atomic occupation, bond lengths and bond angles of NiO with a standard cubic (Fm-3m) symmetry.

a (Å)	b (Å)	c (Å)	V (Å^3)	χ^2	Rp	Rwp
4.229880	4.229880	4.229880	75.68	6.441	1.79	2.25

Atom	Wyckoff Position	X	Y	Z	Occupancy
Ni	4b	0.500000	0.500000	0.500000	1.0000
O	4a	0.000000	0.000000	0.000000	1.0000

Bonding Atom	Bond Length (Å)	Bonding Atom	Bond Angles (°)
Ni-O	2.1149(5)	O-Ni-O	180.00(0)
		O-Ni-O	90.00(0)
		Ni-O-Ni	180.00(0)
		Ni-O-Ni	90.00(0)

Table S2. Lattice parameters, cell volume, agreement factor, atomic coordinates, atomic occupation, bond lengths and bond angles of 0.5P-NiO with a standard cubic (Fm-3m) symmetry.

a (Å)	b (Å)	c (Å)	V (Å^3)	χ^2	Rp	Rwp
4.20746	4.20746	4.20746	74.48	9.38	2.37	3.23

Atom	Wyckoff Position	X	Y	Z	Occupancy
Ni	4b	0.500000	0.500000	0.500000	1.0000
O	4a	0.000000	0.000000	0.000000	0.9786
P	4a	0.000000	0.000000	0.000000	0.0214

Bonding Atom	Bond Length (Å)	Bonding Atom	Bond Angles (°)
Ni-O	2.10372(30)	O(P)-Ni-O(P)	180.00(0)
Ni-P	2.10372(30)	O(P)-Ni-O(P)	90.00(0)
		Ni-O(P)-Ni	180.00(0)
		Ni-O(P)-Ni	90.00(0)
		O-Ni-P	0.00(0)

Table S3. Lattice parameters, cell volume, agreement factor, atomic coordinates, atomic occupation, bond lengths and bond angles of 1P-NiO with a standard cubic (Fm-3m) symmetry.

a (Å)	b (Å)	c (Å)	V (Å^3)	χ^2	Rp	Rwp
4.201662	4.201662	4.201662	74.18	7.32	2.43	3.07

Atom	Wyckoff Position	X	Y	Z	Occupancy
Ni	4b	0.500000	0.500000	0.500000	1.0000
O	4a	0.000000	0.000000	0.000000	0.9616
P	4a	0.000000	0.000000	0.000000	0.0384

Bonding Atom	Bond Length (Å)	Bonding Atom	Bond Angles (°)
Ni-O	2.10083(25)	O(P)-Ni-O(P)	180.00(0)
Ni-P	2.10083(25)	O(P)-Ni-O(P)	90.00(0)
		Ni-O(P)-Ni	180.00(0)
		Ni-O(P)-Ni	90.00(0)
		O-Ni-P	0.00(0)

Table S4. Lattice parameters, cell volume, agreement factor, atomic coordinates, atomic occupation, bond lengths and bond angles of 1.5P-NiO with a standard cubic (Fm-3m) symmetry.

a (Å)	b (Å)	c (Å)	V (Å^3)	χ^2	Rp	Rwp
4.200460	4.200460	4.200460	74.11	9.31	2.65	3.38

Atom	Wyckoff Position	X	Y	Z	Occupancy
Ni	4b	0.500000	0.500000	0.500000	1.0000
O	4a	0.000000	0.000000	0.000000	0.9080
P	4a	0.000000	0.000000	0.000000	0.0920

Bonding Atom	Bond Length (Å)	Bonding Atom	Bond Angles (°)
Ni-O	2.10023(28)	O(P)-Ni-O(P)	180.00(0)
Ni-P	2.10023(28)	O(P)-Ni-O(P)	90.00(0)
		Ni-O(P)-Ni	180.00(0)
		Ni-O(P)-Ni	90.00(0)
		O-Ni-P	0.00(0)

Table S5. Lattice parameters, cell volume, agreement factor, atomic coordinates, atomic occupation, bond lengths and bond angles of 2P-NiO with a standard cubic (Fm-3m) symmetry.

a (Å)	b (Å)	c (Å)	V (Å^3)	χ^2	Rp	Rwp
4.211271	4.211271	4.211271	74.68	8.705	2.06	2.64

Atom	Wyckoff Position	X	Y	Z	Occupancy
Ni	4b	0.500000	0.500000	0.500000	1.0000
O	4a	0.000000	0.000000	0.000000	0.8875
P	4a	0.000000	0.000000	0.000000	0.1125

Bonding Atom	Bond Length (Å)	Bonding Atom	Bond Angles (°)
Ni-O	2.10564(26)	O(P)-Ni-O(P)	180.00(0)
Ni-P	2.10564(26)	O(P)-Ni-O(P)	90.00(0)
		Ni-O(P)-Ni	180.00(0)
		Ni-O(P)-Ni	90.00(0)
		O-Ni-P	0.00(0)

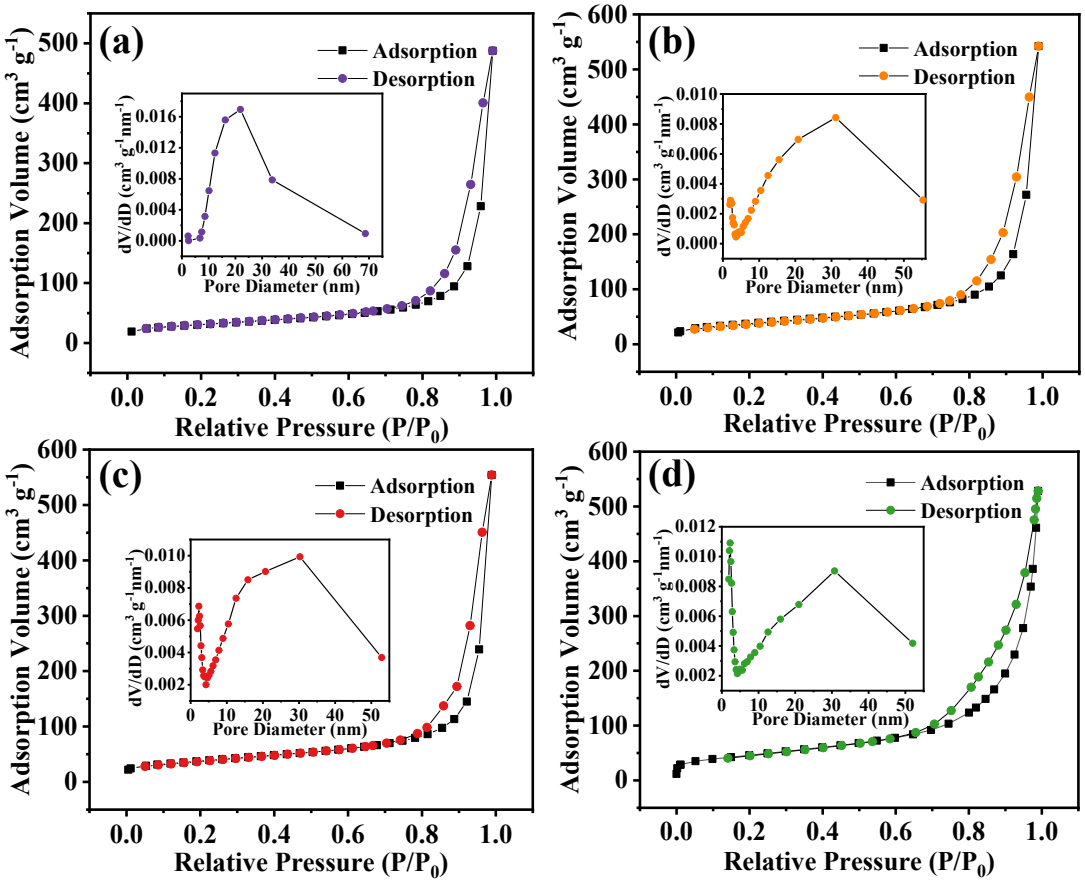

Fig. S10. Nitrogen adsorption/desorption isotherms and pore-size distributions (inset) of (a) NiO, (b) 0.5P-NiO, (c) 1P-NiO and (d) 1.5P-NiO.

Table S6. BET and BJH results of NiO and P-NiO samples.

Sample	**BET Surface Area** ($m^2\ g^{-1}$)	**Pore Volume** ($cm^3\ g^{-1}$)
NiO	108.15	0.753198
0.5P-NiO	134.14	0.838874
1P-NiO	134.63	0.857078
1.5P-NiO	165.09	0.817038
2P-NiO	171.60	0.952739

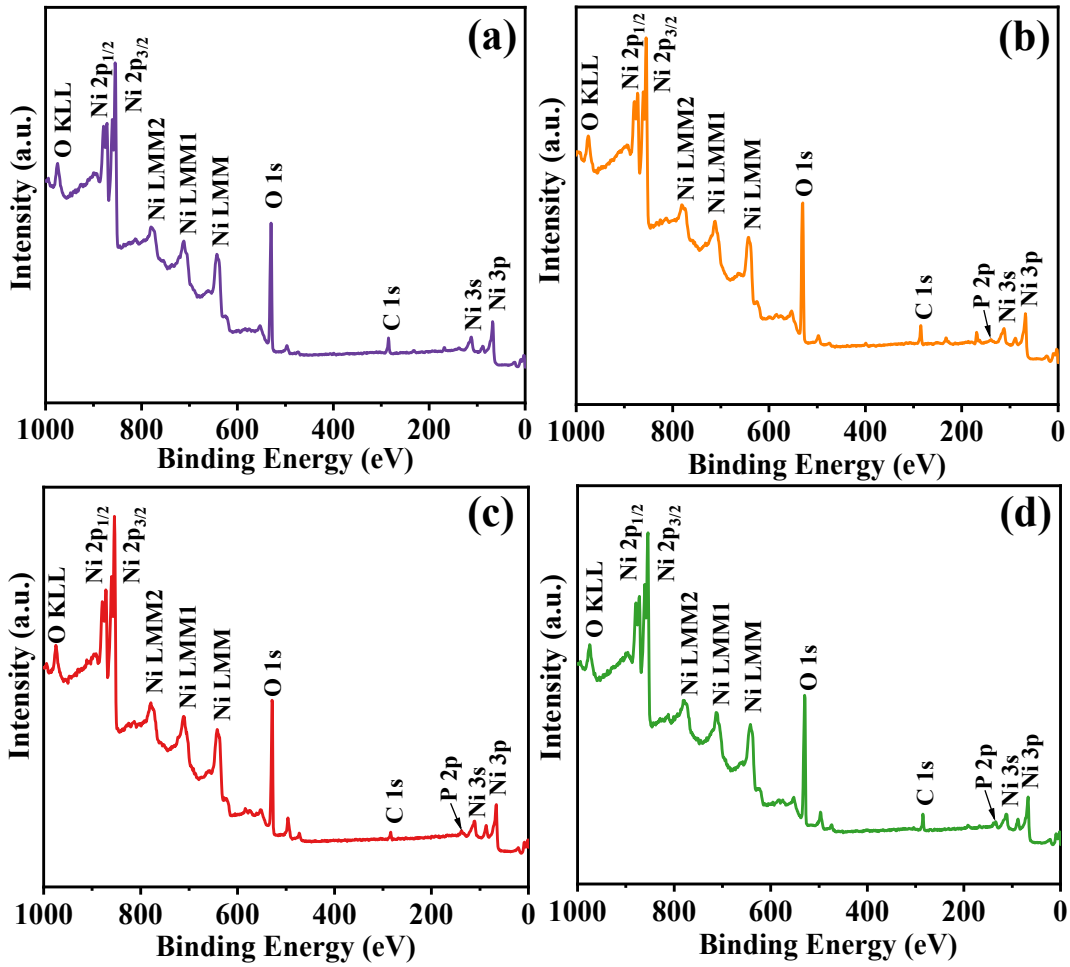

Fig. S11. XPS survey spectra of (a) NiO, (b) 0.5P-NiO, (c) 1P-NiO and (d) 1.5P-NiO.

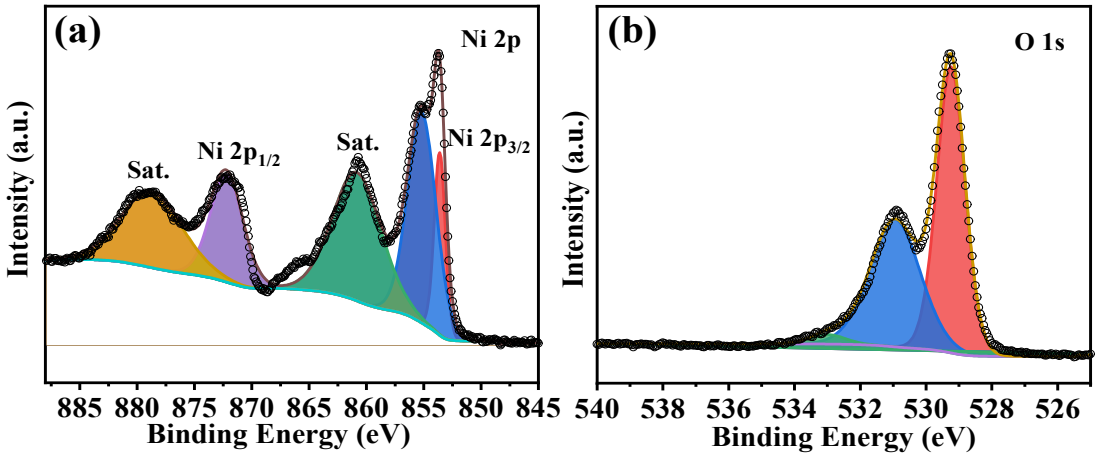

Fig. S12. High-resolution XPS spectra of (a) Ni 2p and (b) O 1s of NiO.

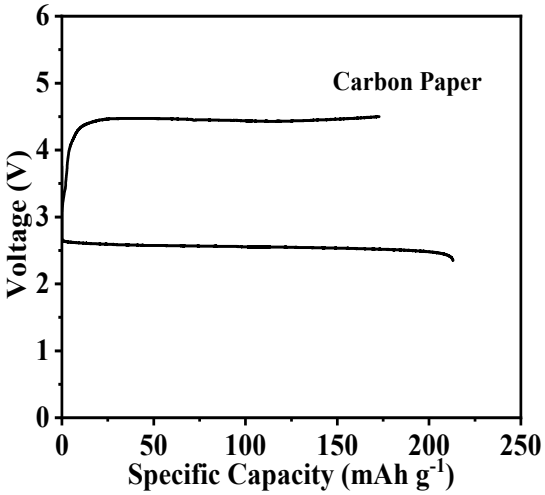

Fig. S13. Galvanostatic discharge-charge curve of pure carbon paper cathode at 100 mA g^{-1}.

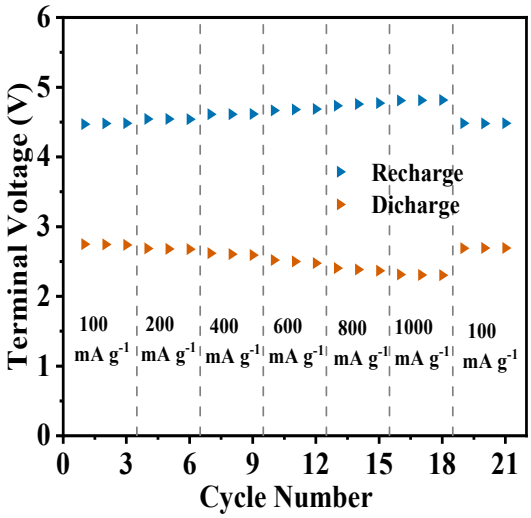

Fig. S14. Rate capability with terminal voltages of 2P-NiO cathode at various current densities ranging from 100 to 1000 mA g^{-1} with the limited specific capacity of 1000 mAh g^{-1}.

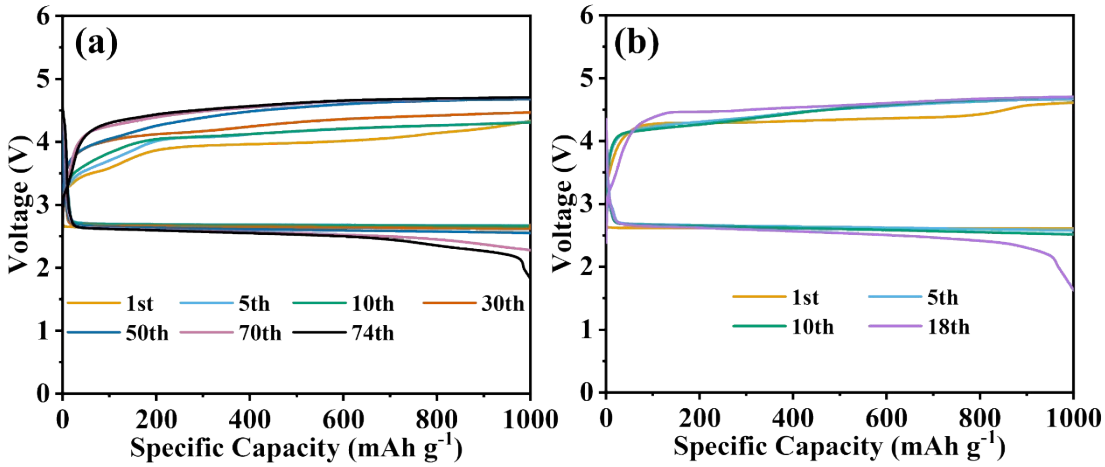

Fig. S15. Cycling performance of (a) NiO and (b) KB cathodes with selected typical discharge/charge profiles under a capacity limit of 1000 mAh g^{-1} at 200 mA g^{-1}.

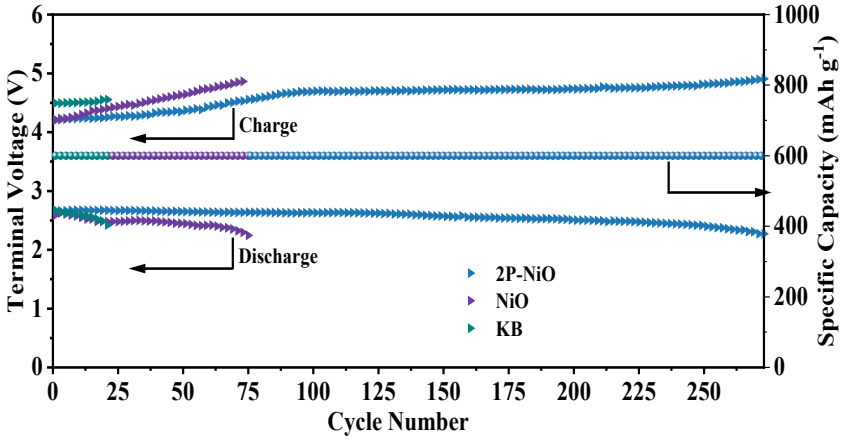

Fig. S16. Cycling performance of different cathodes with corresponding cycle numbers with terminal voltages under a capacity limit of 600 mAh g^{-1} at 200 mA g^{-1}.

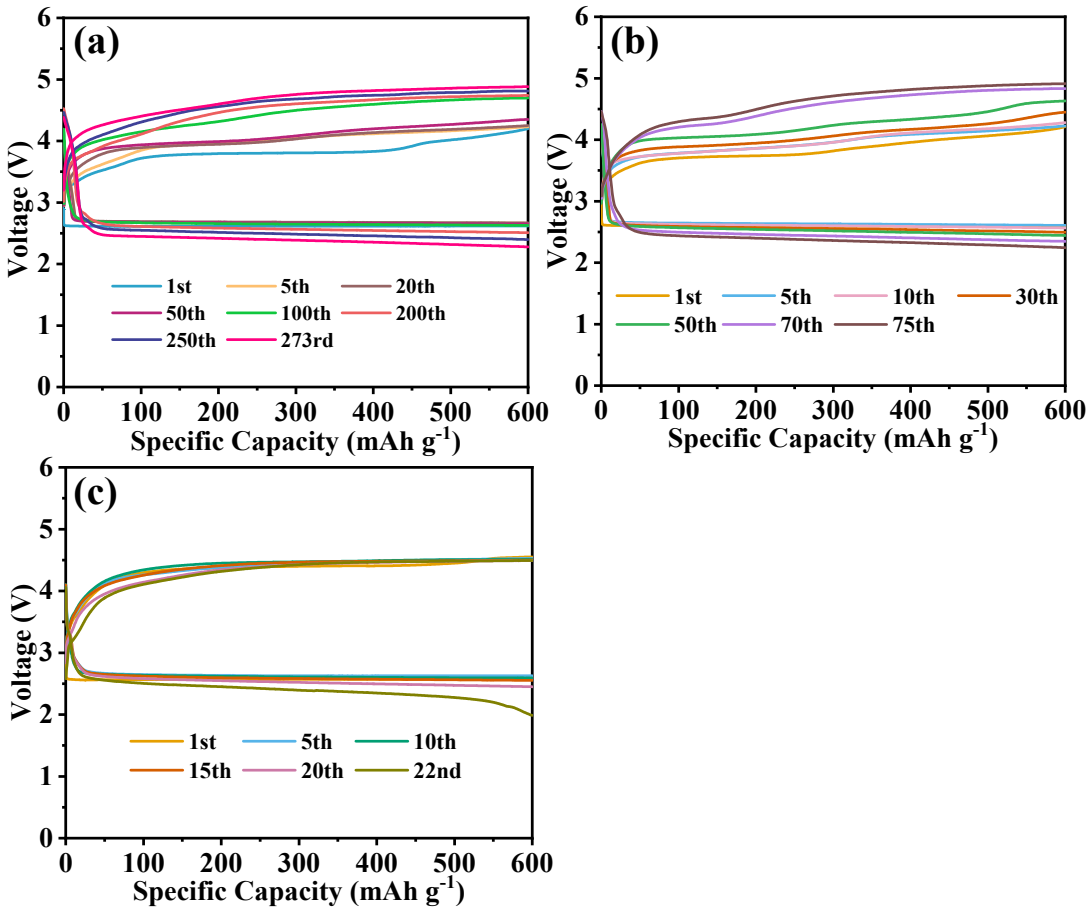

Fig. S17. Cycling performance of (a) 2P-NiO, (b) NiO and (c) KB cathodes with selected typical discharge/charge profiles under a capacity limit of 600 mAh g^{-1} at 200 mA g^{-1}.

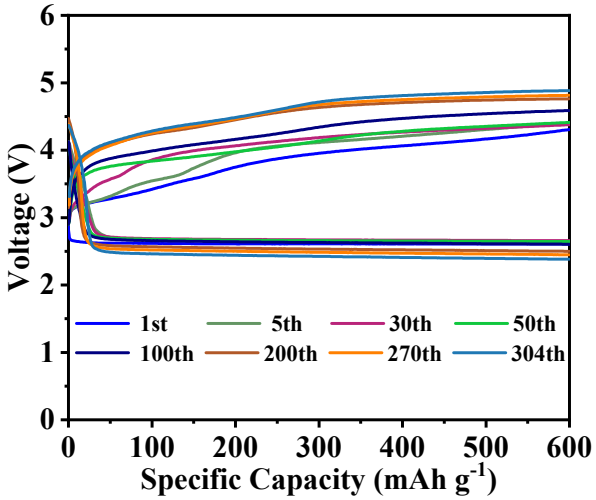

Fig. S18. Selected typical discharge/charge profiles of 2P-NiO cathode under a capacity limit of 600 mAh g^{-1} at 500 mA g^{-1}.

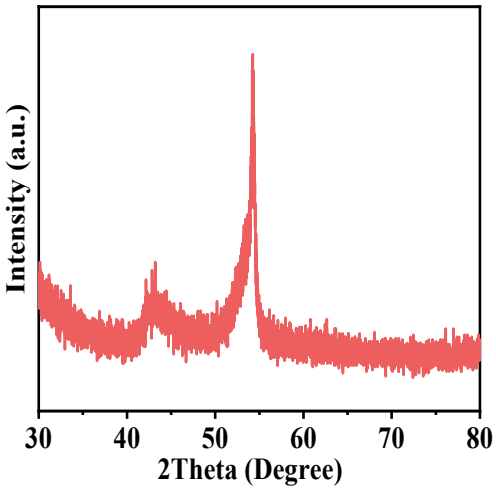

Fig. S19. XRD pattern of carbon

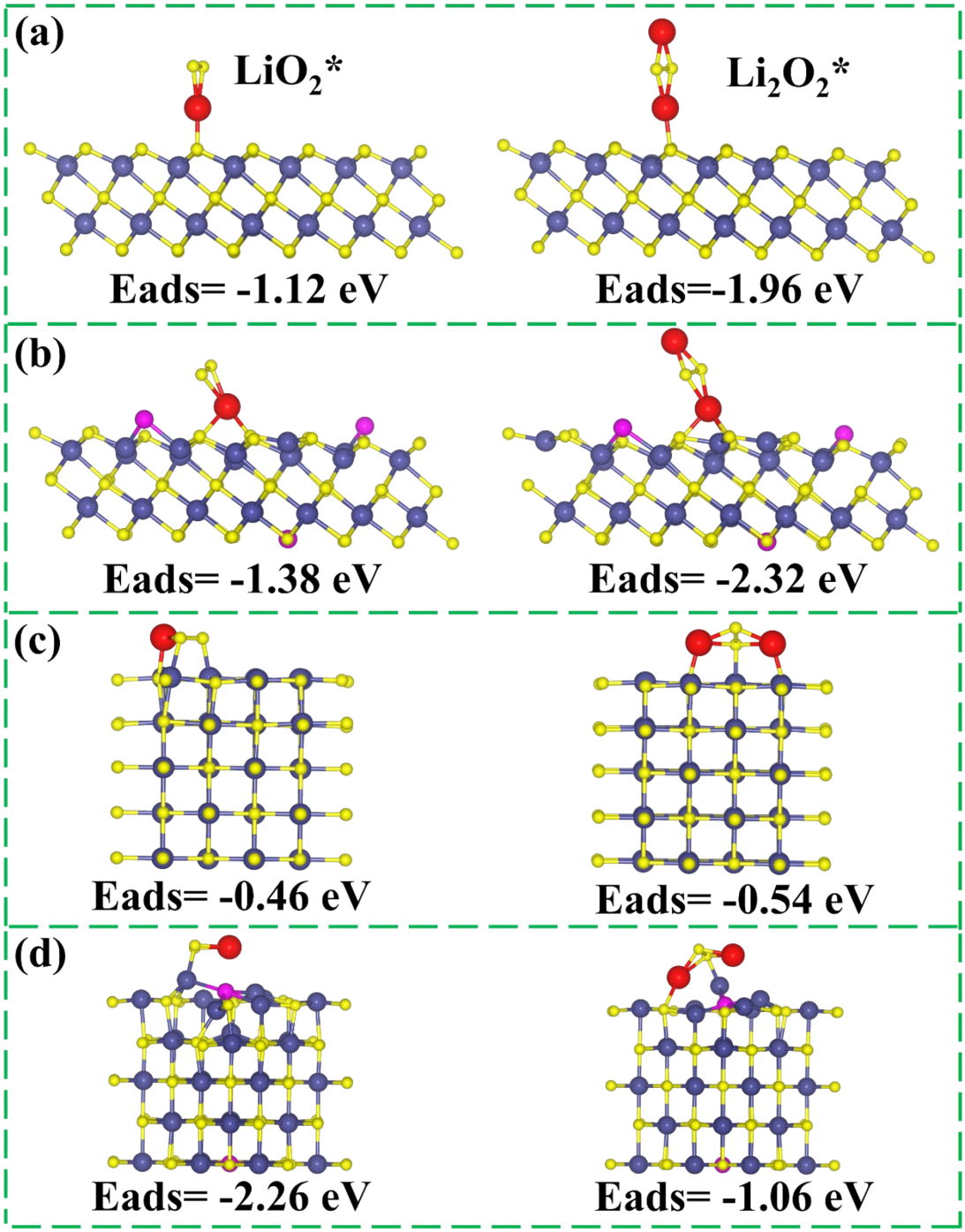

Fig. S20. Optimized structures and adsorption energies (Eads) of LiO_2 and Li_2O_2 adsorbed on the (111) and (100) surfaces for (a), (c) NiO and (b), (d) P-NiO.

Table S7. Bader charge analysis for LiO_2/Li_2O_2-adsorbed NiO and P-NiO, LiO_2/Li_2O_2 adsorbed energy and distance between LiO_2/Li_2O_2 and surface of substrates.

	Substrate-LiO_2			**Substrate-Li_2O_2**		
	Q(liO_2)	R (Å)	Eads (eV)	Q(li_2O_2)	R (Å)	Eads (eV)
NiO (111)	-0.587	3.199	-1.12	-0.801	3.696	-1.96
P-NiO (111)	-0.631	2.510	-1.38	-0.832	3.098	-2.32
NiO (100)	-0.205	1.896	-0.46	-0.332	2.123	-0.54
P-NiO (100)	-0.198	2.708	-2.26	-0.452	2.578	-1.06

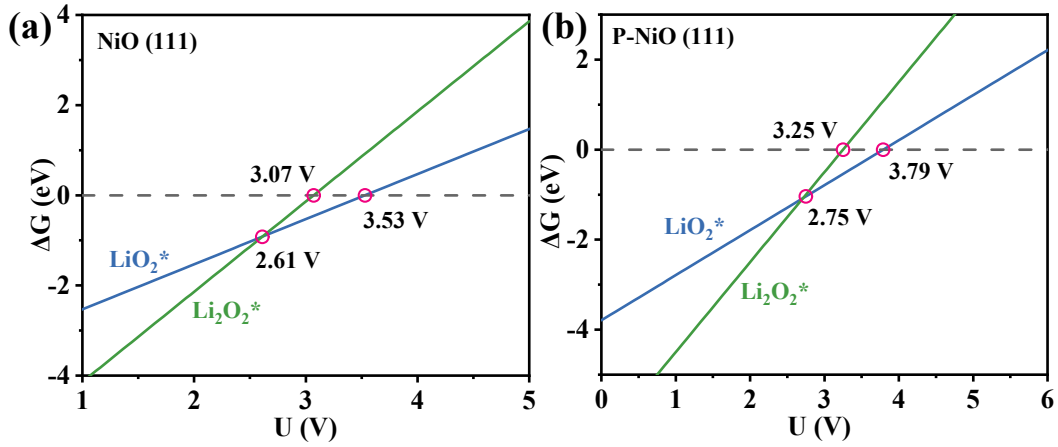

Fig. S21. Phase diagrams of the cathode reaction on (a) NiO and (b) P-NiO (111) planes.

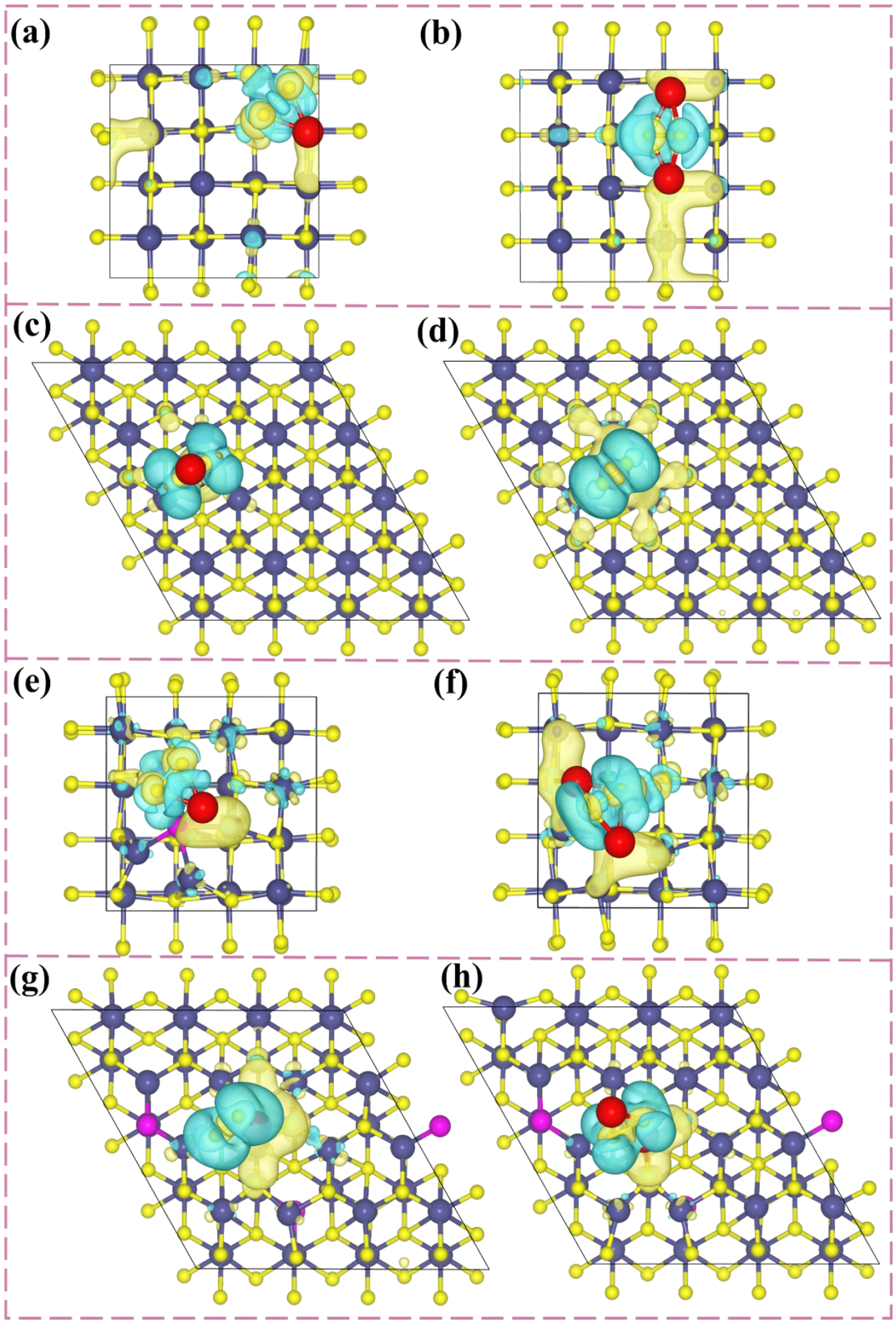

Fig. S22. Contour plots of the differential in charge density for the optimized structures of LiO_2 and Li_2O_2 molecules adsorbed on (a-b) NiO (100), (c-d) NiO (111) and (e-f) P-NiO (100), (g-h) P-NiO (111).

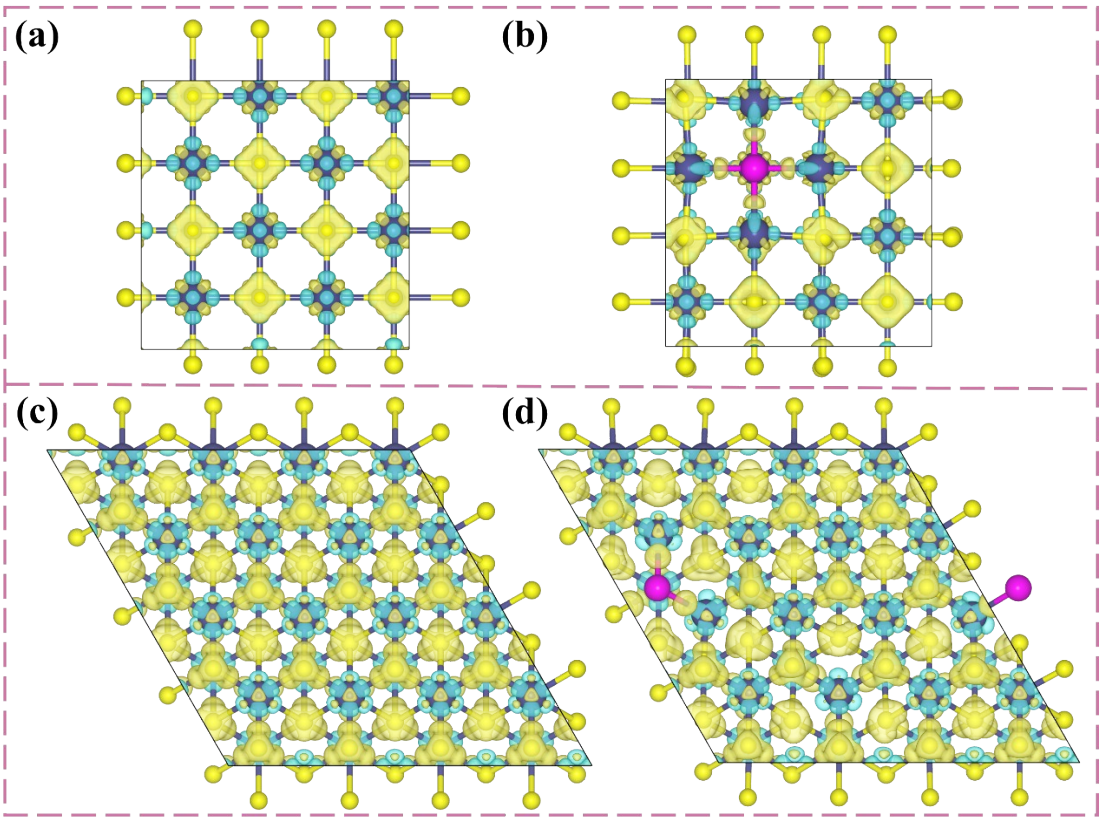

Fig. S23. Contour plots of the differential in charge density for (a) NiO (100), (c) NiO (111) and (b) P-NiO (100), (d) P-NiO (111).